The Utilization of a Multi-Layer Perceptron Model for Estimation of the Heating Load

Ken Chen[1], Wenyao Zhu[2]*
Zhejiang Rongqe Technology Co.Ltd. Zhejiang, 323000, China[1]
Department of Computer Science and Technology, Lishui University, Zhejiang, 323000, China[2]

***Abstract*—The growing significance of energy-efficient building management techniques has led to research that combines precise heating demand predictions with sophisticated optimization algorithms. This research seeks a comprehensive solution to enhance building energy efficiency, addressing the growing concern for sustainability and responsible resource use in contemporary research and practice. In this research endeavor, the complex topic of energy optimization within the complex domain of heating, ventilation, and air conditioning (HVAC) systems is being tackled with a combination of creative problem-solving techniques and thorough examination. The significance of accurate heating load forecasts for raising HVAC system efficiency and cutting expenses is emphasized in this study. It introduces innovative methods by combining two advanced optimization algorithms, the Artificial Hummingbird Algorithm (AHA) and the Improved Arithmetic Optimization Algorithm (IAOA), with the Multi-Layer Perceptron (MLP) model. The main objective is to improve heating load forecast accuracy and expedite HVAC system optimization procedures. This study emphasizes how important precise heating load forecasts are to attaining energy efficiency, cost savings, and the ultimate objective of encouraging environmental sustainability in building management. The assessments unequivocally illustrate that the MLAH (Multi-Layer Perceptron with Artificial Hummingbird Algorithm) model in the second layer emerges as the most exceptional predictor. It attains an impressive maximum Coefficient of Determination (R^2) value of 0.998 during the testing phase, reflecting a remarkable explanatory capacity and displaying remarkably low Root Mean Squared Error (RMSE) and Mean Absolute Error (MAE) values of 0.43 and 0.337, indicating minimal prediction discrepancies compared to alternative models.**

Keywords*—Heating energy consumption; heating load; Multi-Layer Perceptron; Artificial Hummingbird Algorithm; Improved Arithmetic Optimization Algorithm

I. INTRODUCTION

There has been a noticeable surge in academic interest directed toward research projects centered on enhancing buildings' energy efficiency in recent times [1]. This heightened scholarly attention can be traced back to the escalating worries regarding the inefficient consumption of energy resources, along with the long-lasting adverse effects on the environment that this inefficiency brings about [2]. Academics have come to acknowledge the pivotal role played by buildings in the context of energy consumption and the release of greenhouse gases. As a result, they have been diligently investigating various approaches to improve the efficiency of buildings while simultaneously working to reduce their ecological footprint [3].

Achieving energy conservation in buildings requires a comprehensive approach that strongly emphasizes accurately predicting energy usage. This renewed focus has gained recognition and drives the creation of effective energy-saving initiatives. Precise prediction entails meticulous monitoring of energy consumption patterns in buildings. Beyond immediate energy savings, it provides insights into complex dynamics within different building types, enabling tailored strategies for enhanced energy efficiency, whether in residential, commercial, or industrial structures. Accurate energy usage forecasting conserves energy and fosters a sustainable, energy-efficient built environment. This aligns with broader goals of environmental preservation and responsible resource management. By prioritizing precise prediction and targeted energy-saving strategies, progress is made toward a future where buildings are energy-efficient and environmentally conscious, promoting sustainable resource use [4]. Advanced building energy management strategies depend on a deep understanding of energy consumption estimation, including intelligent control systems, fault detection, and demand-side tactics [5], [6]. These techniques use predictive insights to optimize energy use, reduce waste, and ensure efficient building system operation, significantly contributing to improved energy efficiency and overall building functionality. Research has shown that even minor improvements in energy consumption prediction can lead to significant energy savings. Building managers and occupants are empowered by accurate forecasting to make informed decisions, proactively adjust HVAC, lighting, and equipment settings, and adopt energy-saving behaviors. These advanced strategies represent a crucial step toward sustainable and efficient building operations, fostering a culture of responsible energy use [7]. As these methods continue to be developed and implemented, a future is moved closer to where buildings are energy-efficient and adaptive to changing energy demands, benefiting both the environment and occupants [8].

Precisely anticipating energy consumption in buildings constitutes a critical element of energy modeling, yet frequently falls short in replicating real-world outcomes, as demonstrated by various studies revealing substantial disparities between forecasts and actual usage, at times magnifying initial estimates by two or threefold. Conventional energy models, rooted in fundamental physical principles, are well-suited for preliminary assessments but grapple with the intricacies of practical scenarios [9], [10]. To tackle these constraints, numerical simulation techniques come into play, permitting the simulation of building energy utilization and the integration of machine learning models for energy efficiency. Artificial intelligence (AI) models are central in estimating and augmenting building

energy consumption, drawing from historical dataset and real-time sensor inputs. Essentially, merging AI and numerical simulation methods signifies a notable advancement in achieving more precise energy consumption prognostications in building contexts [11], [12]. This strategy, which embraces the complexities of real-world situations, lays the groundwork for effective and flexible energy management, ultimately elevating energy efficiency and advocating for environmental sustainability.

In recent years, significant advancements have been made in energy consumption estimation, driven by the dedication of scholars and experts [13], [14]. This progress is crucial for enhancing energy efficiency and informed decision-making in various applications, particularly in building energy management [15], [16]. A range of machine learning methods, which encompassed KNN, DNN, RF, ANN, GBM, Stacking, SVM, DT, and LR, to forecast the annual energy consumption of residential buildings, were investigated in STUDY [17]. Their study demonstrated that, among these methods, DNN emerged as the most proficient estimative model for estimating energy consumption, particularly during the preliminary design phase. The prediction of Cooling and Heating Loads was the focus of the distinct investigation prepared by [18], employing SVR and MLP models. Impressive results were obtained, with an outstanding R-value of 0.9993 achieved for Heating Load estimation by the MLP model, and the SVR model outstanding with an R-value of 0.9878 in predicting Cooling Load. These findings underscore the precision attainable through machine learning-based approaches. In study [19], researchers looked at the estimation of cooling and heating demands in residential buildings employing fuzzy logic techniques, like the adaptive neural fuzzy inference system (ANFIS) and fuzzy inductive reasoning (FIR). A comparison was made between these fuzzy techniques and thirteen machine learning methods, with SVR, ANFIS, and FIR identified as the superior performers in the research. The estimation of heating energy consumption in Tianjin's residential buildings was explored by [20]. Various algorithms, including SVR, RF, and LGBM, were employed. It was revealed in the findings that the LGBM model outperformed its counterparts in multiple evaluation metrics, thus highlighting its potential for precise energy consumption forecasting. An innovative approach was introduced by study [21], wherein RF and LSTM techniques were integrated to forecast building energy consumption. Remarkably, their method showcased superior performance compared to established benchmark methods, thus emphasizing the potential of hybrid methodologies in energy prediction.

This research aimed to create a machine-learning model that could forecast Heating Load (HL) using information from trustworthy sources. The study used the Multi-Layer Perceptron (MLP) technique to construct strong composite models. These composite models smoothly integrated the Improved Arithmetic Optimization Algorithm (IAOA) and the Artificial Hummingbird Algorithm (AHA) to forecast HL values. MLPs are well-suited for tasks where intricate patterns and interactions exist, which is often the case in heating load prediction, as it involves different factors like building materials, weather conditions, and occupancy patterns. The model's multi-layer architecture and capacity to adapt to diverse data make it a robust choice for accurately estimating heating load, contributing to more efficient HVAC system operations, ultimately leading to energy savings and improved building management.

Enhancements to the current work could involve broadening the scope to integrate real-time data, enabling more dynamic predictions of heating loads. Implementing ensemble methods to amalgamate multiple models could significantly improve predictive accuracy. Furthermore, conducting field trials to validate model performance across varied building environments would bolster its practicality. Introducing feedback mechanisms to iteratively update and refine predictive models using operational data would ensure ongoing efficiency gains. Lastly, exploring enhanced sensor data collection and system monitoring could establish a stronger basis for advancing building energy management in the future.

II. Materials and Methodology

A. Data Processing

The data of the current study have been categorized into several parameters, including Wall Area (WA), Glazing Area Distribution (GAD), Glazing Area (GA), Roof Area (RA), Surface Area (SA), Orientation (Or), Overall Height (OH), and Relative Compactness (RC). Furthermore, the main target of this research is predicting Heating Load (HL). In this study, the dataset was divided into three phases, comprising training (70 percent), validation (15 percent), and testing (15 percent) phases. Dataset division allows for a precise evaluation of the model’s applicability. Numerical summaries of the model’s parameters, offering a comprehensive overview of specific features, including mean values (M), maximum values (Max), minimum values (Min), and standard deviation (St.), are presented in Table I. Based on the data presented in Table I, it is evident that the HL value conforms to precisely defined boundaries, with a firmly established upper limit of 43.1 KW and a precise lower threshold of 6.01 KW, in strict accordance with the specifications of the output parameter.

B. Multi-Layer Perceptron (MLP)

The Multi-layer Perceptron (MLP) stands out as one of the extensively utilized neural network approaches typically trained employing the backpropagation algorithm. The MLP is designed to handle tasks related to asset processes and learning, collectively referred to as the fields of training and estimation. MLP neural networks are renowned for their ability to model intricate and non-linear phenomena in real-world scenarios, thanks to their adaptable approximation capabilities [22].

TABLE I. THE STATISTICAL PROPERTIES OF THE INPUT VARIABLE OF HEATING

Variables		Indicators			
	Category	*Min*	*Max*	*Avg.*	*St. Dev.*
Relative Compactness	***Input***	0.62	0.98	0.76	0.11
Surface Area (m^2)	***Input***	514.50	808.50	671.71	88.09
Wall Area (m^2)	***Input***	245.00	416.50	318.50	43.63
Roof Area (m^2)	***Input***	110.25	220.50	176.60	45.17
Overall Height (m)	***Input***	3.50	7.00	5.25	1.75
Orientation	***Input***	2.0	5.00	3.50	1.12
Glazing Area (%)	***Input***	0.0	0.40	0.23	0.13
Glazing Area Distribution	***Input***	0.0	5.00	2.81	1.55
Heating (KW)	***Output***	6.01	43.10	22.31	10.09

The MLP architecture comprises three interconnected layers: input, hidden, and output. The input layer contains nodes corresponding to the number of predictor variables. Furthermore, a single hidden layer within the MLP can effectively capture highly complex functions through its hidden neurons. Possessing too few neurons can lead to suboptimal neural network performance. Conversely, MLP neural networks are challenging to train and susceptible to overfitting. An MLP neural network is used as $X \in R^D \rightarrow Y \in R^1$, where Y and X represent the output and input parameters, respectively, to generalize the modeling of the non-linear function (h) when employing a single predictor. The number of nodes in the output layer is associated with the variables that are modeled. Eq. (1) represents the function (h):

$$Y = h(X) = s_2 + M_2 \times (k_b(s_1 + M_1 \times X)) \quad (1)$$

k_b serves as the activation function.

s_1 and s_2 denote the bias vectors for the hidden and output layers, respectively.

M_1 and M_2 represent the alternating weight matrices of the hidden and output layers.

The tan-sigmoid and log-sigmoid activation functions find broad application, and their corresponding equations have been specified as Eq. (2) and Eq. (3), alternatively:

$$h_b(T) = \frac{1}{1+\exp(-T)} \quad (2)$$

$$h_b(T) = \frac{\exp(T)-\exp(-T)}{\exp(T)+\exp(-T)} \quad (3)$$

T represents the activation function applied to the input.

C. Artificial Hummingbird Algorithm (AHA)

The flight and foraging behaviors of hummingbirds inspire the Artificial Hummingbird Optimization Approach (AHA). It seeks to replicate the efficient motion patterns of hummingbirds to optimize complex functions. Details about the AHA algorithm can be found in [23]. Eq. (4) explains how the AHA algorithm starts with the establishment of an initial hummingbird population.

$$X_i = L + r \times (U - L), i = 1,2, \dots, N \quad (4)$$

For a d-dimensional exploration space, U and L signify the upper and lower boundaries, respectively.

r denoted a random vector with values uniformly distributed between $[0,1]$.

Eq. (5) is used to create the visit table, which is intended to document the food sources that hummingbirds visit while foraging.

$$VT_{ij} = \begin{cases} 0 & if\ i \neq j \\ null & if\ i = j' \end{cases}, \quad i = 1, \dots, N\ ,\ j = 1, \dots, N \quad (5)$$

If $i = j$, the value $VT_{ij} = null$ denotes the food taken by hummingbird i at its specific food source. Conversely, if $i \neq j$, the value $VT_{ij} = 0$ reflects that hummingbird i has been to the food source at position j without ingesting any food.

1) Guided foraging: Three types of flight skills mentioned before are utilized during the AHA algorithm's searching part. The axial flight is characterized by Eq. (6):

$$D_i = \begin{cases} 1 & if\ i = rand_i([1,d]) \\ 0 & else \end{cases}, \quad i = 1, \dots, d\ , \quad (6)$$

Eq. (7) provides a mathematical representation of the diagonal flight in the AHA algorithm.

$$D_i = \begin{cases} 1 & if\ i = P(i),\ j \in [1,k],\ P = randperm(k), k \in [2, r_1(d-2)+1] \\ 0 & else \end{cases} \quad (7)$$

r_1 denoted a random number.

$randperm(k)$ determines a random permutation of integers in $[1-k]$,

The directed foraging behavior in the AHA algorithm is expressed mathematically in the following:

The AHA algorithm's mathematical representation of the omnidirectional flight skill is formulated as Eq. (8).

$$D_i = 1, i = 1, \dots, d \quad (8)$$

$rand_i$ stands for a random integer in $[1-d]$,

$$V_i(t+1) = X_{i,t}(t) + a \times D \times \left(X_i(t) - X_{i,t}(t)\right), a \in N(0,1) \quad (9)$$

At iteration t,$X_{i,t}(t)$ signifies the food source i.

The food source that the $i-th$ hummingbird visits is $X_{i,t}(t)$.

Eq. (10) may be used to update the value of X_i:

$$X_i(t+1) = \begin{cases} X_i(t) & if\ f(X_i(t) \le f(V_i(t+1)) \\ V_i(t+1) & otherwise \end{cases} \quad (10)$$

f indicates the fitness value of a particular solution or candidate solution.

2) Territorial foraging: Hummingbirds exhibit territorial foraging behavior within their territory, exploring nearby areas for potentially better solutions. This behavior is also incorporated into the guided foraging module of the AHA algorithm, as outlined by Eq. (11):

$$V_i(t+1) = X_{i,t}(t) + b \times D \times X_i(t), b \in N(0,1) \quad (11)$$

3) Migration foraging: This section provides insights into the hummingbird's transition from a food source with a low nectar-refilling rate to a newly generated food source, chosen randomly during its foraging behavior:

$$X_\omega(t+1) = L + r \times (U - L) \quad (12)$$

X_ω reflects the food source with the worst fitness value.

D. Improved Arithmetic optimization algorithm (IAOA)

1) Initialization phase: The initial phase in AOA's optimization process entails generating a collection of candidate solutions (denoted as $\boldsymbol{X}$) through random means. In each iteration, the objective is to pinpoint the most promising candidate solution, with the expectation that it either represents the optimal solution or closely approximates it within a neighboring range.

$$X = \begin{bmatrix} x_{1,1} & \cdots & x_{1,j} & \cdots & x_{1,n} \\ \cdots & \cdots & \cdots & \cdots & \cdots \\ x_{i,1} & \cdots & x_{i,j} & \cdots & x_{i,n} \\ \cdots & \cdots & \cdots & \cdots & \cdots \\ x_{N,1} & \cdots & x_{N,j} & \cdots & x_{N,n} \end{bmatrix} \quad (13)$$

Before initiating the AOA procedure, a decision must be made to determine whether to commence with the exploration or exploitation phases. Subsequently, the Math Optimizer Accelerated (MOA) function, which signifies the function value at the $i-th$ iteration, is computed in accordance with Eq. (14).

$$MOA(C_{It}) = Min + C_{It} \times \left(\frac{Max - Min}{M_{It}}\right) \quad (14)$$

M_{It} signifies the maximum number of iterations.

Max and Min indicated as the highest and lowest values of the accelerated function, respectively.

2) Exploration phase: The exploration phase encompasses mathematical computations employing Division (DO) or Multiplication (MO) operators, yielding outcomes or decisions that are broadly dispersed. These operations may not efficiently approach the target and might only converge toward a nearly optimal solution after several iterations, thus facilitating the transition to the exploitation phase. Eq. (15) delineates the two primary search strategies employed during exploration and furnishes equations for updating positions.

$$x'_{i,j} = \begin{cases} x_{b,j} \div (MOP + \varepsilon) \times \left(\left(UB_j - LB_j\right) \times \mu + LB_j\right), r2 < 0.5 \\ x_{b,j} \times MOP \times \left(\left(UB_j - LB_j\right) \times \mu + LB_j\right), otherwise \end{cases} \quad (15)$$

$x'_{i,j}$ indicates the $j-th$ position of the $i-th$ solution.

ε is a small integer number,

$x_{b,j}$ denotes the $j-th$ position within the currently best-acquired solution.

μ signifies a control parameter.

$MOP(C_{Iter})$ is represented as follows:

$$MOP(C_{It}) = 1 - \left(\frac{C_{It}}{M_{It}}\right)^{1/\alpha} \quad (16)$$

α reflects a critical parameter that controls the precision achieved during the exploitation process across successive iterations.

3) Exploitation phase: Mathematical calculations in the exploitation phase employ Subtraction (SO) and Addition (AO) operators, leading to concentrated outcomes. These operators enable effective targeting of the desired goal across multiple iterations. Eq. (17) outlines the primary search strategies and provides position update equations for this phase. Using these exploitation operators (SO and AO) prevents the system from becoming stuck in local search areas, thereby assisting in discovering optimal solutions within related search approaches.

$$x'_{i,j} = \begin{cases} x_{b,j} - MOP \times \left(\left(UB_j - LB_j\right) \times \mu + LB_j\right), r_3 > 0.5 \\ x_{b,j} + MOP \times \left(\left(UB_j - LB_j\right) \times \mu + LB_j\right), otherwise \end{cases} \quad (17)$$

r_3 refers to a pseudorandom number that is uniformly distributed between $[0,1]$.

4) Improved AOA (IAOA): Kaveh and Biabani Hamedani developed an improved version called the Improved Architecture Optimization Algorithm (IAOA) [24].

On the other hand, close bounds result in small steps, increasing the risk of premature convergence to suboptimal solutions. The original AOA faces a significant issue if all design variables have identical bounds, as in discrete structural optimization with standard sections. Eq. (16) demonstrates that in each iteration, if $r_2 > 0.5$, every aspect of the best solution that has been discovered is adjusted in the same way

$(MOP + \varepsilon) \times \left((UBj - LBj) \times \mu + LBj\right)$. Likewise, if $r_2 \leq 0.5$, each design variable in the best solution discovered to date is scaled by an identical factor $MOP \times ((UBj - LBj) \times \mu + LBj)$. In the original AOA's exploration phase, all design variables in the best solution are altered by two factors, restricting exploration to a narrow space. This limits diversity, causing slow and early convergence to suboptimal solutions [24]. The original AOA also faces this limitation in its exploitation phase (as seen in Eq. 17). To overcome these issues in its exploration phase, a new position updating rule using division and multiplication operators has been introduced in IAOA [24].

$$x'_{i,j} = \begin{cases} x_{i,j} \div (1 + (-1)^{randi([1,2])} \times 0.5 \times rand \times \overline{MOP}, r_2 > 0.5 \\ x_{i,j} \times (1 + (-1)^{randi([1,2])} \times 0.5 \times rand \times \overline{MOP}, otherwise \end{cases} \quad (18)$$

$rand$ denotes a pseudorandom number that follows a uniform distribution in$[0 - 1]$.

$x'_{i,j}$ represents the present value of the $j - th$ design variable for the $i - th$ candidate solution.

$randi([1,2])$ makes a pseudorandom scalar integer, which can be either 1 or 2.

$\overline{MOP}$ is a parameter-free version of the function MOP, which is defined as follows [24]:

$\overline{MOP}$ is a variant of the *MOP* function that does not rely on additional parameters and is defined as described in the study [27].

$$\overline{MOP}(C_{It}) = (1 - \frac{C_{It}}{M_{It}})^{randi([1,2])} \quad (19)$$

In contrast to the original AOA, IAOA's exploration phase focuses on the current solution positions, as shown in Eq. (18). Essentially, in IAOA's exploration phase, each solution's position is adjusted based on its current state. This method promotes a comprehensive search space exploration and avoids the loss of diversity during the search [24]. In addition, the incorporation of random numbers in Eq. (18) and Eq. (19) lead to the creation of different step sizes for relocating solutions within the search space. This variation in step sizes can encourage exploration and maintain the population's diversity [24]. It is worth mentioning that Eq. (18) is not influenced by the limits of design variables, which could potentially alleviate convergence-related problems. [24]. IAOA introduces a new position updating rule for the exploitation phase, using subtraction and addition operators to overcome this limitation [24]:

$$x'_{i,j} = \begin{cases} best(x_j) - best(x_j) \times rand \times \overline{MOP} \times (UB_j - LB_j), r_3 > 0.5 \\ best(x_j) + best(x_j) \times rand \times \overline{MOP} \times (UB_j - LB_j), otherwise \end{cases} \quad (20)$$

Eq. (19) and Eq. (20) create variable step sizes for solution movement, improving the utilization of the best solution. In contrast, the original AOA necessitates tuning four specific parameters (Min, Max, α, and μ) for each application. Remarkably, IAOA simplifies this process by removing α and μ from its formulation, making it a more straightforward implementation. Fig. 1 shows the flowchart of IAOA.

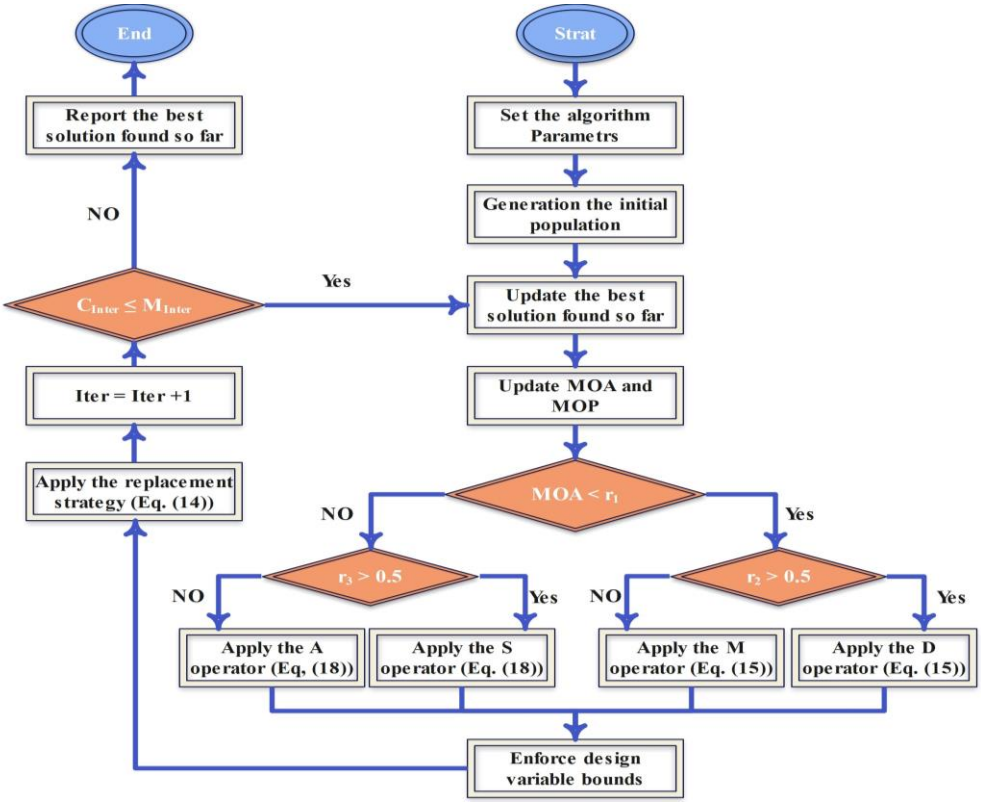

Fig. 1. Flowchart of IAOA.

E. Performance Evaluation Methods

A range of evaluators, mainly concentrating on accurately measuring correlations and errors, were employed to assess the applicability of hybrid models. The metrics are Coefficient of Determination (R^2), Root Mean Squared Error (RMSE), Mean Absolute Error (MAE), n10_index, and Normalized Mean Square Error (NMSE). These metrics serve as essential instruments for assessing the performance of hybrid models in diverse scenarios, offering valuable insights into the accuracy and reliability of their predictions.

$$R^2 = \left(\frac{\sum_{i=1}^{N}(p_i-\bar{p})(s_i-\bar{s})}{\sqrt{[\sum_{i=1}^{N}(p_i-\bar{s})^2][\sum_{i=1}^{N}(s_i-\bar{s})^2]}} \right)^2 \quad (21)$$

$$RMSE = \sqrt{\frac{1}{N}\sum_{i=1}^{N}(s_i - p_i)^2} \quad (22)$$

$$MAE = \frac{1}{N}\sum_{i=1}^{N}|s_i - p_i| \quad (23)$$

$$n10 - index = \frac{n10}{N} \quad (24)$$

$$NMSE = \frac{1}{N}\sum_{i=1}^{N}\frac{(p_i-s_i)^2}{s_i.p_i} \quad (25)$$

In the above equations, N defines the numbers associated with the samples, s_i defines the estimated value, $\bar{s}$ defines the mean of the estimated values, p_i defines the experimental value and $\bar{p}$ defines the experimental amount's average.

F. Significant of Research

The research discussed holds significant implications for advancing energy-efficient building management practices, particularly in the context of HVAC systems. By integrating advanced optimization algorithms and accurate heating load forecasting, the study addresses critical challenges in enhancing building energy efficiency. This is crucial in the face of mounting global concerns over sustainability and responsible resource use. Firstly, the study's focus on combining the Artificial Hummingbird Algorithm and the Improved Arithmetic Optimization Algorithm with a Multi-Layer Perceptron model represents a cutting-edge approach in HVAC system optimization. These algorithms offer innovative solutions to the complex problem of energy optimization, aiming to streamline processes and minimize energy wastage. Secondly, the emphasis on precise heating load predictions is pivotal for optimizing HVAC operations. Accurate predictions not only lead to improved system efficiency but also contribute to substantial cost savings by reducing energy consumption and operational inefficiencies. Moreover, by enhancing predictive accuracy, the research directly supports efforts to mitigate environmental impact associated with building operations, aligning with global sustainability goals. Furthermore, the study's findings highlight the MLAH model's exceptional performance in predicting heating loads, showcasing its potential to outperform traditional models. Achieving a high R^2 value of 0.998 during testing underscores its reliability and robustness in real-world applications. Generally, this research determines the critical role of advanced methodologies in driving progress towards sustainable building practices.

III. Results

As described in previous sections, in this study, two hybrid models, including the combination of the MLP model with two distinct optimization systems (AHA and IAOA), were generated to predict Heating Load (HL) values. The outcomes of the prediction processes are summarized in Table II. A total of five metrics were utilized to evaluate the models' performance. The interpretation of the results is described as follows:

A. Coefficient of Determination (R^2)

The R^2 values consistently show higher values in the testing phase when compared to both the validation and training phases across all models. This consistent trend suggests that the models were sufficiently trained, leading to their optimal performance in subsequent phases. Notably, during the testing phase, the second layer of the MLAH model outperformed the other models, achieving an impressive R^2 value of 0.998, firmly establishing itself as the top-performing model. In contrast, the first layer of the MLIA model performed less effectively, with an R^2 value of 0.965, making it the least successful model in this study.

B. Root Mean Squared Error (RMSE)

Among the models examined, the MLAH model's second layer demonstrated the lowest RMSE value, surpassing others by 0.43 in the testing phase, confirming its position as the most accurate model in terms of prediction. In contrast, the MLIA model's first layer, with an RMSE value of 1.895, emerged as the least effective among the models, indicating its relatively weaker predictive performance.

C. Mean Absolute Error (MAE)

As indicated in Table II, the second layer of the MLAH model stood out as the top performer among all the models, exhibiting lower MAE values. To provide more detail, the MLAH model achieved the most favorable MAE value, measuring 0.337. In contrast, the MLIA model produced the least favorable outcome, with the highest MAE value of 1.398 among all the models. This difference in MAE values emphasizes the superior predictive precision of the second layer of the MLAH model when compared to the other choices.

D. Normalized Mean Square Error (NMSE)

The MLAH model in the second layer outperformed the other models. The NMSE values varied, with the second layer of the MLAH model achieving a minimum of 0.002 and the first layer of the MLIA model reaching a maximum of 0.025 among all the models. This variation in NMSE values highlights that the first layer of the MLIA model exhibited a broader range of uncertainty in its predictions compared to the other options.

E. n10_index

In the testing phase, the MLAH2 model achieved the highest n10_index value of 1.0, establishing itself as the top-performing model among all those under examination. Conversely, the MLIA1 model was identified as the least effective, recording the lowest n10_index value of 0.822. This disparity in n10_index values underscores the MLAH2 model's superior estimative accuracy in contrast to the comparatively lower performance of the MLIA1 model.

TABLE II. THE RESULT OF DEVELOPED MODELS FOR MLP

	Model	Phase	Index values				
			RMSE	***R^2***	***MAE***	***n10_index***	***NMSE***
Layer 1 1	**MLAH**	***Train***	1.635	0.975	1.198	0.822	0.005
		Validation	1.390	0.980	1.032	0.904	0.017
		Test	1.371	0.982	1.066	0.878	0.016
		All	1.563	0.977	1.153	0.842	0.003
	MLIA	***Train***	1.895	0.965	1.398	0.755	0.007
		Validation	1.227	0.985	0.939	0.887	0.013
		Test	1.702	0.972	1.368	0.774	0.025
		All	1.782	0.969	1.325	0.777	0.004
Layer 2	**MLAH**	***Train***	1.073	0.989	0.702	0.935	0.002
		Validation	0.625	0.996	0.384	0.991	0.003
		Test	0.430	0.998	0.337	1.000	0.002
		All	0.945	0.991	0.600	0.953	0.001
	MLIA	***Train***	1.516	0.978	0.915	0.896	0.004
		Validation	1.161	0.986	0.630	0.913	0.012
		Test	0.917	0.992	0.531	0.948	0.007
		All	1.392	0.981	0.815	0.906	0.003
Layer 3	**MLAH**	***Train***	1.238	0.985	0.784	0.859	0.003
		Validation	0.932	0.991	0.607	0.939	0.008
		Test	0.937	0.991	0.575	0.948	0.008
		All	1.155	0.987	0.726	0.884	0.002
	MLIA	***Train***	1.652	0.974	1.222	0.827	0.005
		Validation	1.302	0.983	0.989	0.904	0.015
		Test	1.449	0.979	1.028	0.851	0.018
		All	1.574	0.976	1.158	0.842	0.003

In Fig. 2, scatter plots illustrate the connection between predicted and observed HL values, with a specific emphasis on assessing RMSE and R^2 metrics. RMSE, which reflects the dispersion of data points, diminishes as accuracy improves, while R^2 pulls data points closer to the central axis. A total of six models (MLAH and MLIA in three layers) were generated by merging the MLP model with two optimization techniques across the testing, validation, and training phases. Fig. 2 serves as a visual summary of the outcomes, clearly highlighting the superior performance of the MLAH hybrid model in the second layer, which combines the MLP approach with the AHA optimizer. This excellence is discernible from the tightly grouped data points that align closely with the central line. Conversely, the figures indicate that the MLIA model in the first layer exhibited the least effective performance, as evident from the numerous data points positioned beyond the reference lines.

Fig. 3 visually compares two models, MLAH and MLIA, across three layers of the MLP method using stacked column plots. The results for three key metrics, R^2, RMSE, and MAE, are briefly summarized. The R^2 plot demonstrates that the MLAH model in the second layer outperformed all other models with an R^2 value of 0.998, signifying its superior performance. It is worth noting that lower values of RMSE and MAE indicate better model performance in terms of error. In this context, the MLIA model in the first layer stands out as the least favorable model, with RMSE and MAE values of 1.895 and 1.398, respectively. Considering all the results, the MLAH model in the second layer emerges as the most accurate model for predicting HL values.

Fig. 4 is a valuable visual representation of error frequencies in the discussed models, demonstrating their stability within an acceptable range, often resembling a bell-shaped curve. Notably, during the rigorous testing phase of the second model iteration, particularly in the MLAH model, a distinct and pronounced peak in error frequency emerges, reaching around 250, demanding scrutiny. Significantly, error frequencies consistently decrease in validation and training phases across all models, resulting in a flatter curve than the training phase, indicating overall model improvement. Significantly, Fig. 4 provides strong evidence of the MLAH hybrid model's superiority, which combines MLP and AHA in its second layer, showcasing exceptional performance and making it the preferred choice among the considered models.

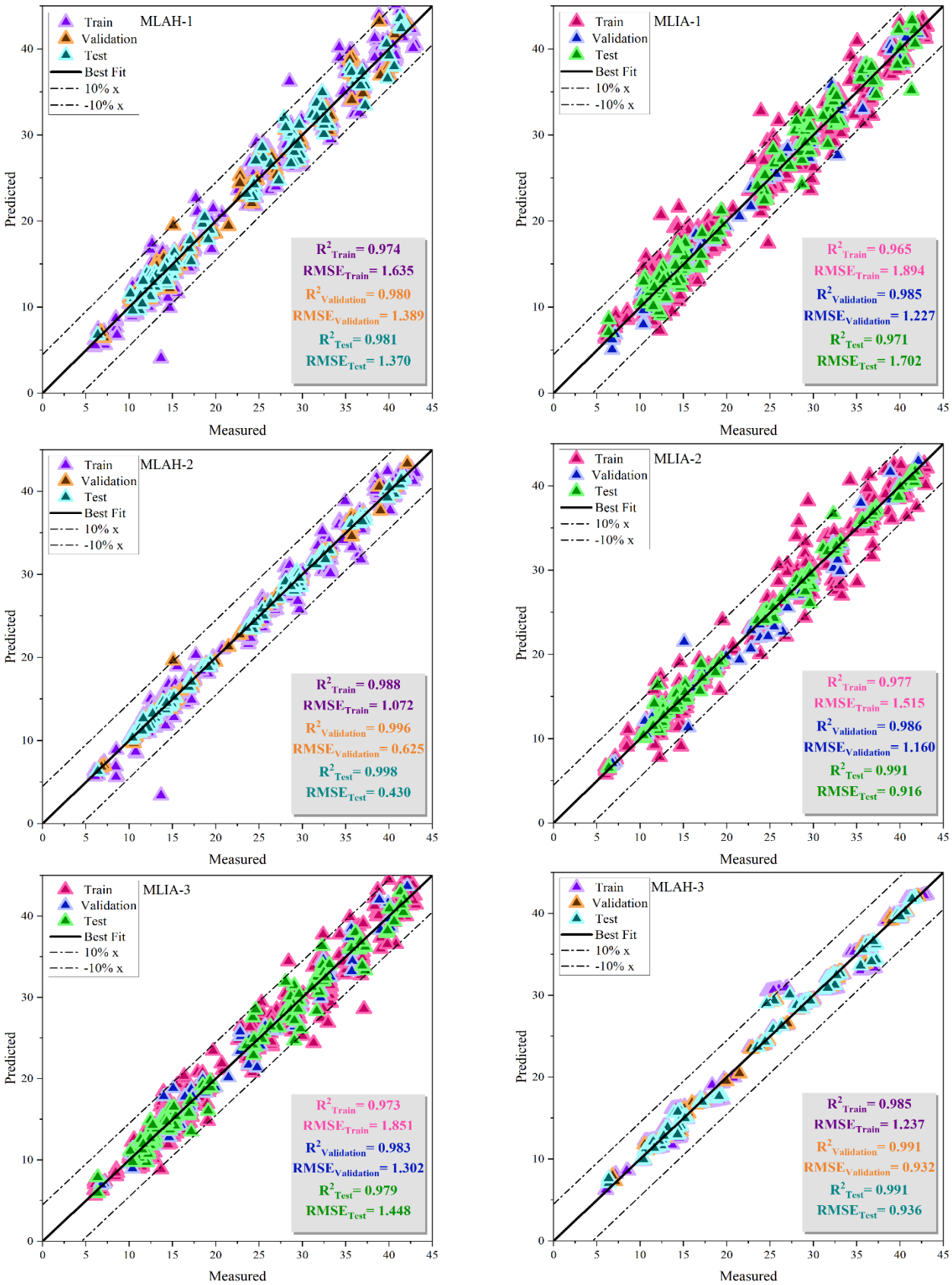

Fig. 2. Plotting the dispersion of evolved hybrid models.

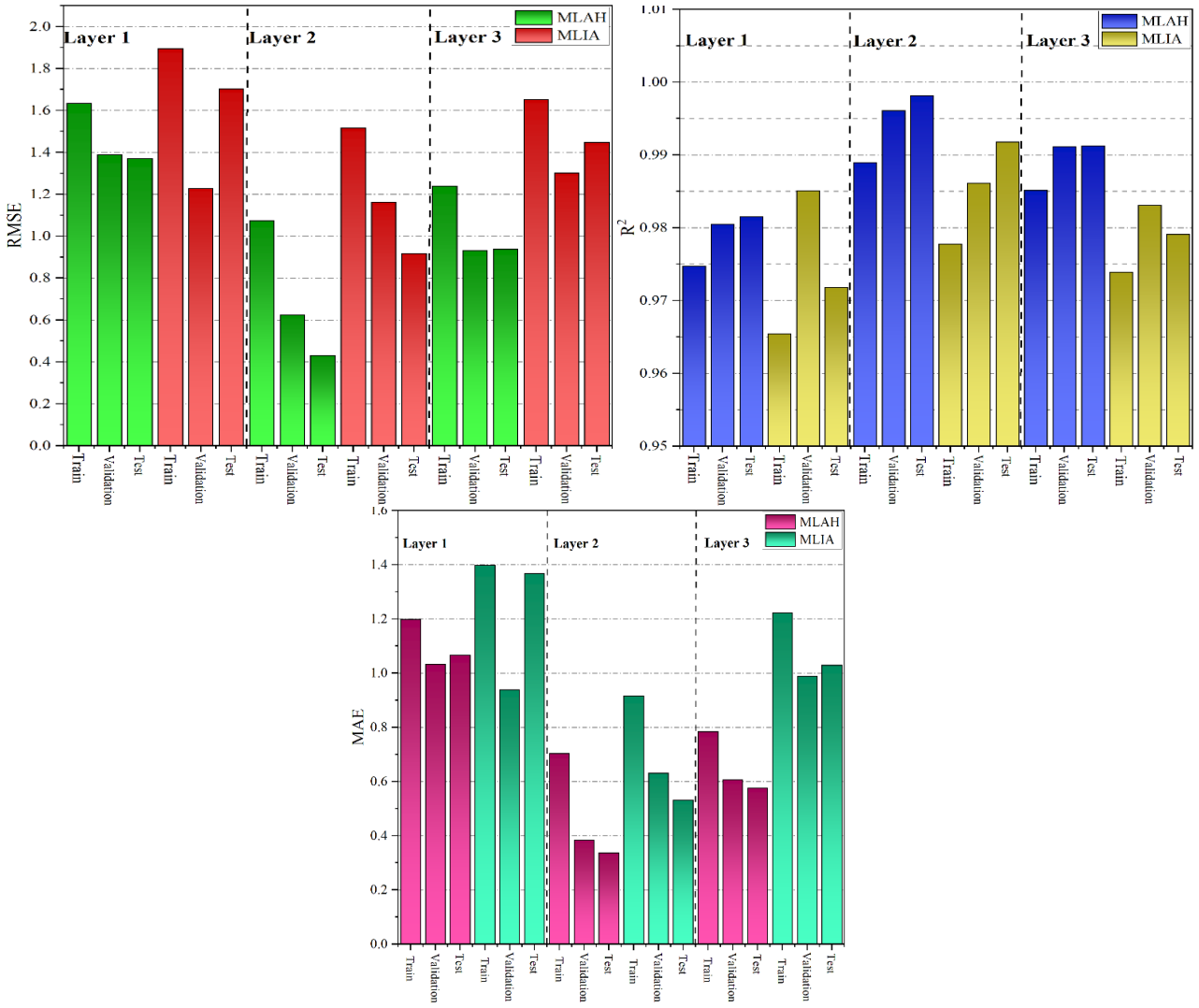

Fig. 3. Stacked column for metric.

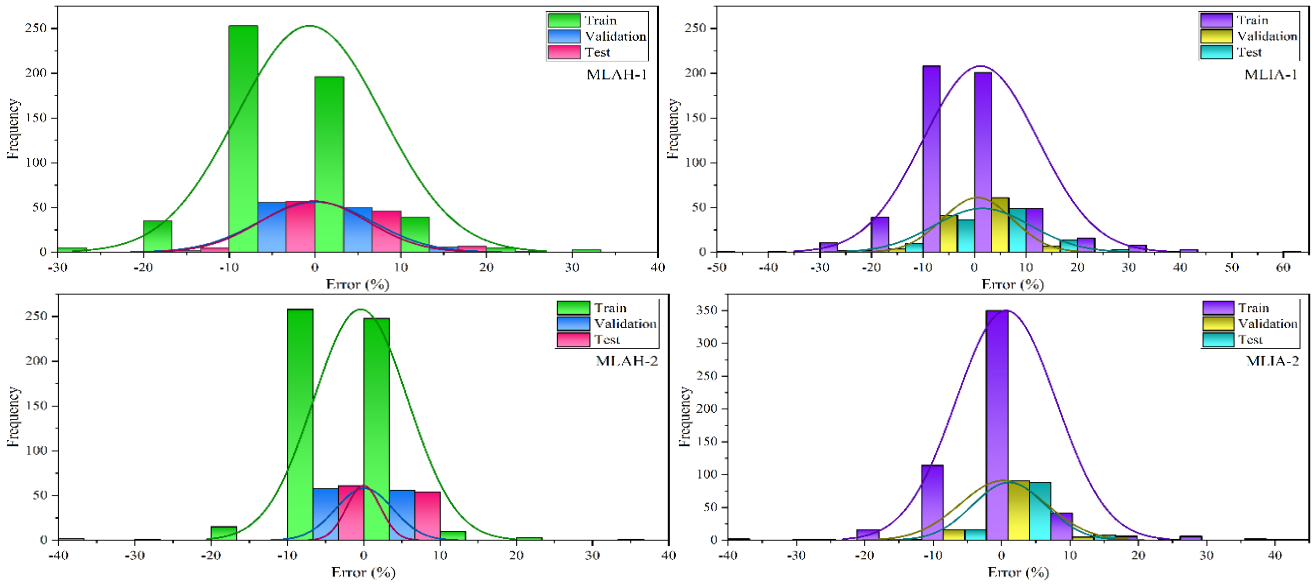

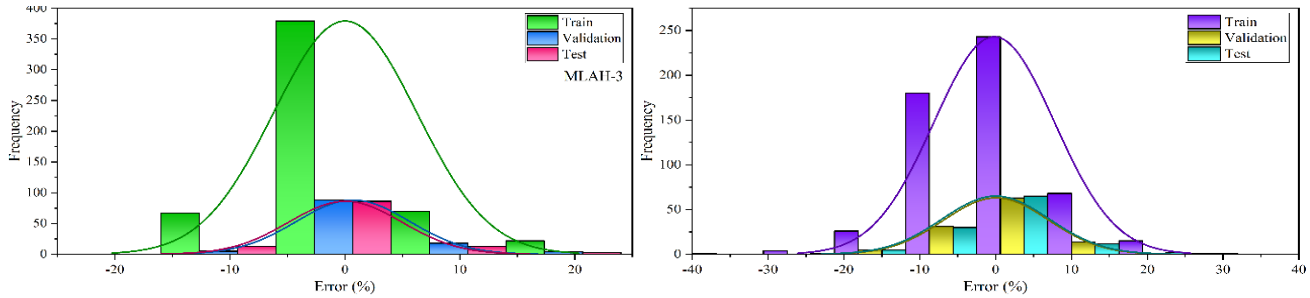

Fig. 4. The error percentage of the models is based on the distribution plot.

Fig. 5 functions as a visual representation, depicting how errors are distributed during the prediction of HL values using two different models across the three layers of the MLP model. Notably, during the training phase in the first layer, the MLIA model exhibited the highest error rates. In contrast, the MLAH model in the second layer consistently demonstrated the lowest error rates. A thorough examination consistently favored the MLAH hybrid model throughout all stages of the study. During the training phase of the first layer in the MLIA model, errors spanned a broad spectrum, ranging from -70 to 40. In contrast, the MLAH model in the second layer, which emerged as the top performer, exhibited errors concentrated within a narrower range of -10 to 10, highlighting its superior predictive accuracy.

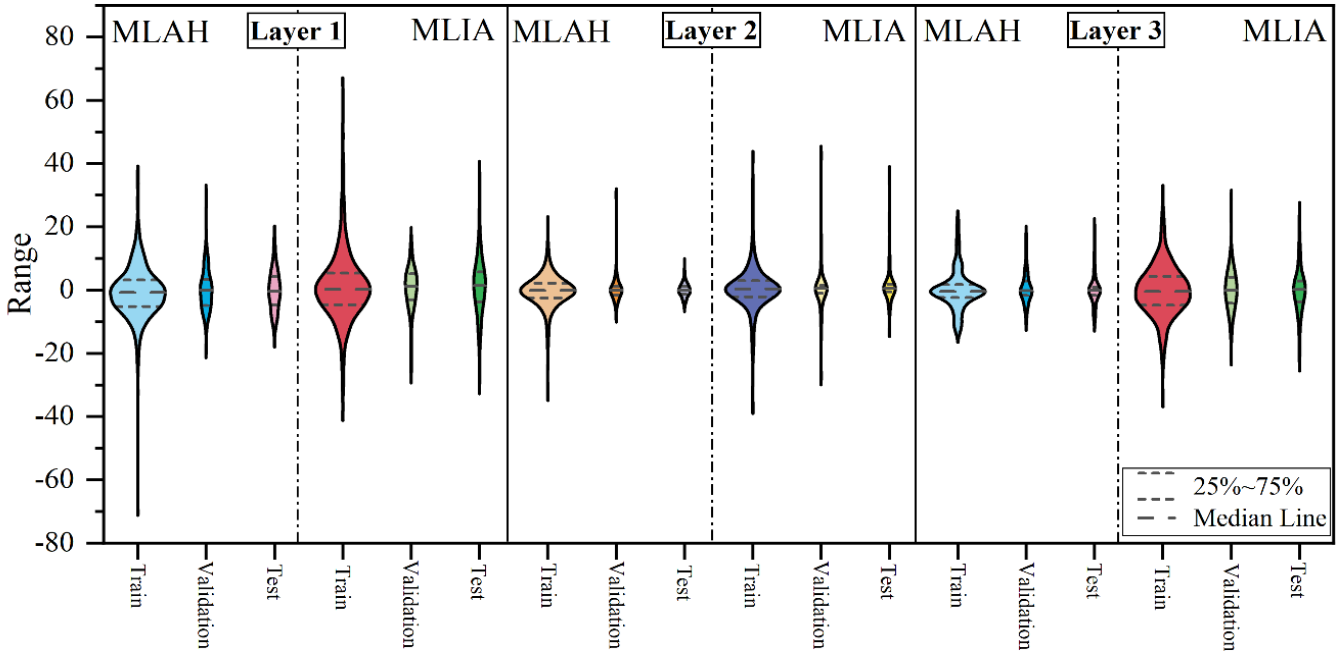

Fig. 5. The violin with quartile errors of proposed models.

IV. Discussion

A. Comparison

Table III show the comparison of the best-performing models in this study with related literature highlights the efficacy of the proposed approach. Moradzadeh et al. [25] employed a Support Vector Regression (SVR) model, achieving an RMSE of 0.483 and an R^2 of 0.997. This indicates a high degree of accuracy, though the RMSE suggests there is room for improvement in minimizing prediction errors. Roy et al. [26] used a Multivariate Polynomial Regression Model (MPMR), which produced an impressive RMSE of 0.059 and an R^2 of 0.99. Despite the excellent RMSE, the slightly lower R^2 value compared to Moradzadeh et al. suggests it explains slightly less variance. Gong et al. [27] applied the Light Gradient Boosting Machine (LGBM) model, resulting in an RMSE of 0.192 and an R^2 of 0.988. This model demonstrates strong predictive performance, but like the others, it falls short in some areas when compared to the present study. The present study's model, MLAH2, stands out with an R^2 of 0.998 and an RMSE of 0.43. While the RMSE is higher than Roy et al.'s MPMR model, the R^2 value of 0.998 indicates a superior ability to explain variance in the data, highlighting the model's overall efficacy. The MLAH2 model's performance underscores the importance of combining advanced optimization algorithms with accurate heating load forecasting to achieve high predictive accuracy and efficiency in HVAC systems. In summary, while each model reviewed has its strengths, the MLAH2 model from the present study demonstrates a balanced and high-performing approach, setting a new benchmark for accuracy in heating load predictions within the field of energy-efficient building management.

TABLE III. THE COMPARISON OF THE BEST PERFORMED MODELS RESULTS OF PRESENT STUDY WITH SOME RELATED LITERATURES

Article	Model	Evaluator	
		RMSE	R^2
Moradzadeh et al. [25]	SVR	0.483	0.997
Roy et al. [26]	MPMR	0.059	0.99
Gong et al. [27]	LGBM	0.192	0.988
Present Study	MLAH2	0.43	0.998

B. Limitation

Enhancing predictive models for Heating Load (HL) prediction offers significant benefits, yet this study has several limitations. The primary limitation lies in the dataset's scope and diversity. The models were trained and tested on a specific dataset, which may not generalize well to different climates, building types, or operational conditions. Thus, the applicability of the findings to broader contexts remains uncertain. Another limitation is the complexity of the optimization algorithms used. Both the Improved Arithmetic Optimization Algorithm (IAOA) and the Artificial Hummingbird Algorithm (AHA) are computationally intensive, which can be a barrier to their practical implementation in real-time applications. The high computational cost might limit their usability in resource-constrained environments. Additionally, while the MLAH model in the second layer showed superior performance, the study did not explore the reasons behind the underperformance of the first layer of the MLIA model. Understanding these reasons could provide valuable insights for refining and improving the models further. Lastly, the models demonstrated a tendency to underestimate HL values, which could have practical implications. This bias towards underestimation needs to be addressed to ensure the models' reliability and accuracy in real-world applications. Future research should focus on expanding the dataset, exploring alternative models, and addressing computational efficiency to overcome these limitations.

V. CONCLUSION

Enhancing predictive models, particularly for Heating Load (HL) prediction, offers significant potential to boost operational efficiency and cost reduction. This study is founded on the Multi-Layer Perceptron (MLP) framework for constructing predictive models. Two optimization algorithms, the Artificial Hummingbird Algorithm (AHA) and the Improved Arithmetic Optimization Algorithm (IAOA), have been seamlessly integrated to enhance model precision and efficiency. The research results validate the effective use of these optimization method in developing accurate estimative models for estimating Heating Load (HL) values. According to the results obtained, it can be inferred that the MLAH model in the second layer of the testing phase distinctly excels in terms of accuracy when compared to the others. This model exhibits exceptional performance, characterized by $RMSE = 0.43$ as the lowest RMSE value and the highest coefficient of determination R^2 value with 0.998. These results unquestionably emphasize the remarkable proficiency of the second layer of the MLAH model in precisely estimating HL values. The first layer of the MLIA model displayed the least favorable performance compared to all the examined models. This was evident in its recording of the highest error value, with 1.895 for the RMSE metric, and the lowest Coefficient of Determination value, with 0.965. The analysis of the measured and estimated values revealed that the models tend to underestimate the HL values, with an average underestimation of approximately 1.5 for the RMSE evaluator. Among these models, the highest error in terms of RMSE was observed in MLIA in the first layer, with an error of 1.895. In contrast, the model MLAH in the second layer exhibited the lowest error, with an error of 0.43 percent.

ACKNOWLEDGMENT

1.Lishui Economic and Technological Development Zone key research and development project Lishui Economic and Technological Development Zone 2022KFQZDYF11(Multi-mission Unmanned aerial Systems in Complex Environments) 2.Public Technology Application Research of Zhejiang Province Natural Science Foundation of Zhejiang Province LGG20F020020 (Research and Development of BIM-3DGIS Photo reality Integrated 3D Online Platform and Key Technology Based on WebGL).

REFERENCES

[1] W. Jin et al., “A novel building energy consumption prediction method using deep reinforcement learning with consideration of fluctuation points,” Journal of Building Engineering, vol. 63, p. 105458, 2023.

[2] B. Sadaghat, S. Afzal, and A. J. Khiavi, “Residential building energy consumption estimation: A novel ensemble and hybrid machine learning approach,” Expert Syst Appl, vol. 251, p. 123934, 2024, doi: https://doi.org/10.1016/j.eswa.2024.123934.

[3] A. Nakhaee Sharif, S. Keshavarz Saleh, S. Afzal, N. Shoja Razavi, M. Fadaei Nasab, and S. Kadaei, “Evaluating and identifying climatic design features in traditional Iranian architecture for energy saving (case study of residential architecture in northwest of Iran),” Complexity, vol. 2022, 2022.

[4] H. Zhong, J. Wang, H. Jia, Y. Mu, and S. Lv, “Vector field-based support vector regression for building energy consumption prediction,” Appl Energy, vol. 242, pp. 403–414, 2019.

[5] D. Darwazeh, J. Duquette, B. Gunay, I. Wilton, and S. Shillinglaw, “Review of peak load management strategies in commercial buildings,” Sustain Cities Soc, vol. 77, p. 103493, 2022.

[6] Y. Zhao, C. Zhang, Y. Zhang, Z. Wang, and J. Li, “A review of data mining technologies in building energy systems: Load prediction, pattern identification, fault detection and diagnosis,” Energy and Built Environment, vol. 1, no. 2, pp. 149–164, 2020.

[7] A. Gellert, U. Fiore, A. Florea, R. Chis, and F. Palmieri, “Forecasting electricity consumption and production in smart homes through statistical methods,” Sustain Cities Soc, vol. 76, p. 103426, 2022.

[8] W. Zhang, Q. Chen, J. Yan, S. Zhang, and J. Xu, “A novel asynchronous deep reinforcement learning model with adaptive early forecasting method and reward incentive mechanism for short-term load forecasting,” Energy, vol. 236, p. 121492, 2021.

[9] J. Runge and R. Zmeureanu, “Forecasting energy use in buildings using artificial neural networks: A review,” Energies (Basel), vol. 12, no. 17, p. 3254, 2019.

[10] B. Sadaghat, A. Javadzade Khiavi, B. Naeim, E. Khajavi, A. R. Taghavi Khanghah, and H. Sadaghat, “The Utilization of a Naïve Bayes Model for Predicting the Energy Consumption of Buildings,” Journal of Artificial Intelligence and System Modelling, vol. 1, no. 01, 2023.

[11] Y. Himeur, K. Ghanem, A. Alsalemi, F. Bensaali, and A. Amira, “Artificial intelligence based anomaly detection of energy consumption in buildings: A review, current trends and new perspectives,” Appl Energy, vol. 287, p. 116601, 2021.

[12] T. Čegovnik, A. Dobrovoljc, J. Povh, M. Rogar, and P. Tomšič, "Electricity consumption prediction using artificial intelligence," Cent Eur J Oper Res, pp. 1–19, 2023.

[13] J. Zhou, Y. Liu, and J. Yi, "Effect of uneven multilane truck loading of multigirder bridges on component reliability," Structural Concrete, vol. 21, no. 4, pp. 1644–1661, 2020.

[14] V. V Mokeev, "Prediction of heating load and cooling load of buildings using neural network," in 2019 International Ural Conference on Electrical Power Engineering (UralCon), IEEE, 2019, pp. 417–421.

[15] J. Song, L. Zhang, G. Xue, Y. Ma, S. Gao, and Q. Jiang, "Predicting hourly heating load in a district heating system based on a hybrid CNN-LSTM model," Energy Build, vol. 243, p. 110998, 2021.

[16] Y. Liu, X. Hu, X. Luo, Y. Zhou, D. Wang, and S. Farah, "Identifying the most significant input parameters for predicting district heating load using an association rule algorithm," J Clean Prod, vol. 275, p. 122984, 2020.

[17] M. Adegoke, A. Hafiz, S. Ajayi, and R. Olu-Ajayi, "Application of Multilayer Extreme Learning Machine for Efficient Building Energy Prediction," Energies (Basel), vol. 15, no. 24, p. 9512, 2022.

[18] A. Moradzadeh, A. Mansour-Saatloo, B. Mohammadi-Ivatloo, and A. Anvari-Moghaddam, "Performance evaluation of two machine learning techniques in heating and cooling loads forecasting of residential buildings," Applied Sciences, vol. 10, no. 11, p. 3829, 2020.

[19] À. Nebot and F. Mugica, "Energy performance forecasting of residential buildings using fuzzy approaches," Applied Sciences, vol. 10, no. 2, p. 720, 2020.

[20] M. Gong, Y. Bai, J. Qin, J. Wang, P. Yang, and S. Wang, "Gradient boosting machine for predicting return temperature of district heating system: A case study for residential buildings in Tianjin," Journal of Building Engineering, vol. 27, p. 100950, 2020.

[21] I. Karijadi and S.-Y. Chou, "A hybrid RF-LSTM based on CEEMDAN for improving the accuracy of building energy consumption prediction," Energy Build, vol. 259, p. 111908, 2022.

[22] H. Moayedi and S. Hayati, "Applicability of a CPT-based neural network solution in predicting load-settlement responses of bored pile," International Journal of Geomechanics, vol. 18, no. 6, p. 6018009, 2018.

[23] W. Zhao, L. Wang, and S. Mirjalili, "Artificial hummingbird algorithm: A new bio-inspired optimizer with its engineering applications," Comput Methods Appl Mech Eng, vol. 388, p. 114194, 2022.

[24] A. Kaveh and K. B. Hamedani, "Improved arithmetic optimization algorithm and its application to discrete structural optimization," in Structures, Elsevier, 2022, pp. 748–764.

[25] A. Moradzadeh, A. Mansour-Saatloo, B. Mohammadi-Ivatloo, and A. Anvari-Moghaddam, "Performance evaluation of two machine learning techniques in heating and cooling loads forecasting of residential buildings," Applied Sciences, vol. 10, no. 11, p. 3829, 2020.

[26] S. S. Roy, P. Samui, I. Nagtode, H. Jain, V. Shivaramakrishnan, and B. Mohammadi-Ivatloo, "Forecasting heating and cooling loads of buildings: A comparative performance analysis," J Ambient Intell Humaniz Comput, vol. 11, pp. 1253–1264, 2020.

[27] M. Gong, Y. Bai, J. Qin, J. Wang, P. Yang, and S. Wang, "Gradient boosting machine for predicting return temperature of district heating system: A case study for residential buildings in Tianjin," Journal of Building Engineering, vol. 27, p. 100950, 2020.